Self-Powered Transformer Eddy Current Damper for Vibration Control of Rotors

Mario Silvagni [*]
Politecnico di Torino,
Department of Mechanical and
Aerospace Engineering -
Mechatronics Laboratory
Torino, ITALY

Andrea Tonoli
Politecnico di Torino,
Department of Mechanical and
Aerospace Engineering -
Mechatronics Laboratory
Torino, ITALY

Angelo Bonfitto
Politecnico di Torino,
Department of Mechanical and
Aerospace Engineering -
Mechatronics Laboratory
Torino, ITALY

Abstract

The vibration control of rotors is usually performed using passive dampers, in layouts where the support of the rotating parts is achieved by rolling-element or hydrodynamic type bearings. Active magnetic bearings could be a promising however they show serious drawbacks, in terms of mass, at least when the generation of strong magnetic forces is required.

Electromagnetic dampers seem a valid alternative to viscoelastic/hydraulic dampers and to active magnetic bearings because their simpler architecture, and, if of transformer type, also for the absence of power electronics, position sensors and any fast feedback loop. However transformer eddy current dampers require a constant voltage power supply (usually based on common power electronics) often integrated with active electronics components. To reduce cost, improve the reliability some applications could benefit a simplified system avoiding active components and providing the required energy with an embedded generator.

The aim of the present paper is to propose a self-powered damper to fulfil these requirements. A three-phase permanent magnet electric generator (connected to the rotating shaft) generates the required power for the damping device. The generator is connected to the damping circuit by means of suitable impedance and a three-phase rectifier.

1   Introduction

The control of rotor vibration is essential in several applications to avoid excessive rotor bend at critical speeds and, in general, to ensure acceptable levels of vibration.

Several solutions have been proposed to this end, many of them (i.e: squeeze film dampers), are passive and usually designed as a compromise for a range of conditions. Their performances are affected by vibration frequency, oil temperature, supply pressure and thermal growth of the bearing housing.

Active/semi-active hydraulic systems have been developed to improve the performances of purely passive solutions. More recently, electro-rheological [1,2] and magneto-rheological [2] semi-active damping systems have shown attractive potential for the adaptation of the damping force to the operating conditions. However, electro-hydraulic, electro-rheological, and magneto-rheological devices cannot avoid drawbacks related to the ageing of the fluid and to the tuning required for the compensation of the temperature and frequency effects. Active Magnetic Bearings (AMB) have therefore received much attention. They offer the greatest possibilities to isolate the rotors from the engine structure and to optimize the system dynamics. The main problem with AMB is that, both static and control forces acting on the rotor must be provided by the electro-mechanical interaction. The static forces are usually much larger than the control ones. The result is that size and mass is often not acceptable for the applications. If the load compensation is supplied by other means, much lighter electro-magnetic actuators can be adopted with the objective of introducing only the requested damping forces. Electromechanical dampers seem to be a valid alternative to visco-elastic and hydraulic ones due to, among others: a) the small sensitivity to the operating conditions, b) the wide possibility of tuning even during operation, and c) the predictability of the behaviour. The advantages of electromechanical damping systems have stimulated considerable research activity during the past decade. The target applications range from the field of rotating machines to that of vehicle suspensions.

*Contact Author Information: mario.silvagni@polito.it, Politecnico di Torino, Department of Mechanical and Aerospace Engineering - Mechatronics Laboratory, C.so Duca degli Abruzzi, 24 10129 Torino, ITALY, Phone:+39 (0)11 0906239, Fax:+39 (0)11 090963

Passive or semi-active eddy current dampers seem to give interesting opportunities in the near term. Compared to active closed loop devices, eddy current dampers have much simpler architecture due to the absence of power electronics and position sensors. They are intrinsically not affected by instability problems due to the absence of a fast feedback loop. Their simple design works well in terms of reliability and lower cost, but limits flexibility and adaptability to the operating conditions. The working principle of eddy current dampers is based on the magnetic interaction generated by magnetic flux linkage variation in a conductor [3] and [4]. Such a variation may be generated using two different strategies:

- moving a conductor in a stationary magnetic field that is variable along the direction of the motion;
- changing the reluctance of a magnetic circuit whose flux is linked to the conductor.

In the first case, the eddy currents in the conductor interact with the magnetic field and generate Lorenz forces proportional to the relative velocity of the conductor itself. Graves, Toncich and Iovenitti [5] defined this kind of damper as "motional" or "Lorentz" type. In the second case, the variation of the reluctance of the magnetic circuit produces a time variation of the magnetic flux. The flux variation induces a current in the voltage driven coil and, therefore, a dissipation of energy. This kind of damper is defined in [6] as the "transformer", or "reluctance" type.

The literature on eddy current dampers is mainly focused on the analysis of "motional" devices. Nagaya in [7] and [8] introduced an analytical approach to describe how damping forces can be exploited using monolithic plane conductors of various shapes. Karnopp and Margolis in [9] and [10] describe how "Lorentz" type eddy current dampers could be adopted as semi-active shock absorbers in automotive suspensions. The application of the same type of eddy current damper in variuos field is described in [11], [12], [13] and [14].

Being usually less efficient than "Lorentz" type, "transformer" eddy current dampers are less common in industrial applications. However, they may be preferred in some areas for their flexibility and construction simplicity. If driven with a constant voltage they operate in passive mode while if current driven they become force actuators to be used in active configurations. A promising application of the "transformer" eddy current damper seems to be its use in aero-engines as a non-rotating damping device in series to a conventional rolling element bearing that is connected to the engine frame with a mechanical flexible support. Similarly to a squeeze film damper, the device acts on the non-rotating part of the bearing. As it is not rotating, there are no eddy currents due to rotation but just to whirling.

In a previous paper [15], the authors presented the mathematical models governing the dynamic behaviour of such devices. The models were validated experimentally on laboratory test rigs. Then, in [16], they show how different electromechanical dampers can be devised for application in a civil aero engine.

As a matter of fact, in several applications, where a high level of reliability and safety is required (i.e: aero engine, chemical/oil and gas industry), the use of open loop system (such as passive or transformer damper) are preferred instead of closed loop system (such as active magnetic bearing/damper) for their intrinsic stability and lower number of active/controlled components. In same applications, the possibility of having a passive, not supplied, device is considered positive. As passive systems are usually hard to design and to operate, the possibility of an active, self-powered system could be a valid alternative.

According to this, the usage of semi active transformed eddy current damper, in which the required power is provided directly with specific subcomponent can lead to a step forward in reliability (less components and subsystems) integration (self-contained and self-powered device) and performances. This aspect seems not being investigated from other authors yet.

The aim of this work is to analyse the characteristic of the self-powered transformer eddy current damper, with a model based approach and provide a methodology to design the system.

The assumptions of the model have been validated on a rotating test rig representing the dynamic behaviour of an aircraft engine.

2 System Description

The present research has been carried on the Rotordynamics Test Rig (RTR), reported as in Figure 1, reproducing the main rotor-dynamic mode shapes of a civil aircraft turbo-engine shaft. The stator has been designed to avoid interaction between its dynamics and that of the rotor so it is not representative of the complexity of a real engine stator; it acts rather as a seismic mass. The rotor and its supports are representative of the bending modes of the Low Pressure (LP) shaft of an aircraft engine. The low pressure turbine and the low pressure compressor are represented by two rigid disks connected by a small diameter hollow shaft that is supported by standard rolling bearing. Both supports are connected to the stator by two sets of bars subject to bending when the rotor moves laterally as in a squirrel cage arrangement.

The main mechanical parameters (such as rotor length and diameter; disks masses, inertia and positions; supports stiffnesses and configuration), have been selected to reproduce the main mode shapes of a low pressure shaft within the rotational speed range of 6000 rpm and the dimensional constraints. The first two critical speeds may occur at about 2000-2500 rpm and 3500-4000 rpm while the third is out of the speed range (about twice the max rotational speed). Following what usually happens in LP shafts of aero-engines, the two first critical speeds involve the bouncing of supports with most of the strain energy associated to them. By converse, the second critical speed involves mostly the LPT support, with most of the energy in it; in both these modes the displacement of the stator (the four rigid columns and connecting plates) is negligible. Additionally, for technological reasons, the vibration amplitude should not exceed 1 mm in the whole speed range to cope with standard range position sensors.

In this paper the self-powered damper is installed only to the support vibrating in the second critical speed while the other support is left undamped. The rotor is spun by commercial permanent magnets brushless electrical motor; the required torque is provided by a small diameter shaft capable of transmitting the torque without adding lateral stiffness that could affect the rotor behaviour.
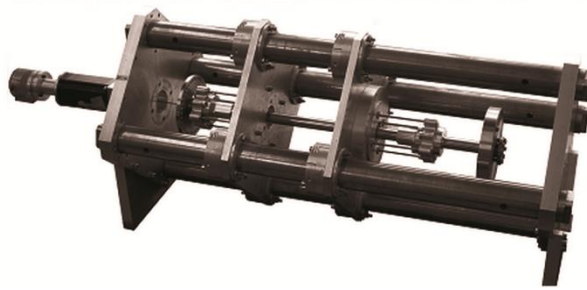
Figure 1: Picture of the Rotordynamics Test Rig (Dampers are not installed)

Figure 2 (for only one of the two supports) shows the system configuration of the self-powered damper [17]. The rotor (1) connected, through the rolling bearing (2) with a supporting spring (6) to the housing (7), as described before. The electromagnetic damping device acts in parallel with the supporting springs. It consists in a set of coils (4), the iron circuit (5) splitted in the static part connected to the housing and the anchor connected to vibrating part, separated by the airgap (3).

An electric generator (8), connected to the rotor, is used to generate the required power for the damping device. A three-phase permanent magnet brushless motor has been employed to this end. The generator is connected to the damping circuit (11) by means of suitable impedance (9) and a three-phase rectifier (10).
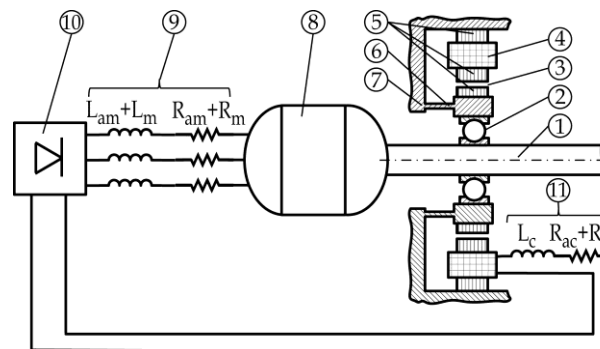
Figure 2: Sketch of the self-powered magnetic damper (power supply on the upper coil is not reported)

The design parameters are (L_{am}, L_m, R_{am}, R_m and R_{ac}) should be designed to optimize the obtainable damping. Qualitatively speaking, as the rotors spin speed increase, the generated voltage rise. The electrical pole of the generator circuit is placed to shape the voltage characteristic in order to limit the damper supply voltage thus to control the amount of damping provided and the power dissipated. Once the desired voltage is achieved (usually while the rotor is crossing its main critical speed), power is no longer increasing while the damping effect is decreasing due to electrical pole of the transformer damper, reducing the mechanical transmissibility. Main parameters of the electromechanical systems are reported in Tables 1 and 2.

Electromagnetic Damper		
Teeth thickness	mm	11
Teeth axial length	mm	35
Inner diameter	mm	50
Outer diameter	mm	100
Overall length	mm	45
Airgap	mm	0.5
Number of turns	-	110
Coil resistance (R_c)	Ω	1.4
Additional resistance (R_{ac})	Ω	2.2
Coil inductance (L_c)	mH	15

Electric generator		
Type	PM External Rotor AXI 4130-20G	
Voltage constant	Rpm/VppL-L	270
Pole pairs	-	7
Winding resistance (R_m)	Ω	0.118
Winding inductance (L_m)	μH	46
Flat Angle BEMF	$^\circ$	40
Additional resistance (R_{am})	Ω	0.09
Additional inductance (L_{am})	μH	560

Table 1: Electromagnetic damper parameters   Table 2: Electric generator parameters

3   Modelling

The full system has been modelled to build a dynamic simulator of the self-powered magnetic damper applied to the rotordynamics test rig. The model is used, in time or frequency domain, for system design, verification and validation. In this section a general description of the system is provided, then the main subsystems are detailed analysed.

3.1   Self-Powered Damper Architecture

The generator is driven by the rotor at the angular speed Ω and produces three phase voltages the are fed to the tuning circuits (Ram, Lam) and then to the three-phase diode rectifier. These are modelled as a R L series and by a diode bridge with 6 diodes. The resulting DC voltage (a stabilizing capacitor is here omitted) supplies the coil set (four coils, two for each axis of the support). The interaction between the supply voltage and the damping force is reported in paragraph 3.3 as the mechanical system of the rotor is explained in paragraph 3.4. Figure 3 shows the block diagram of the system.
The numerical simulator has been developed using Matlab/Simulink. The electrical part is modelled using SimPower toolbox, while the rotor model is derived using Dynort finite element code.
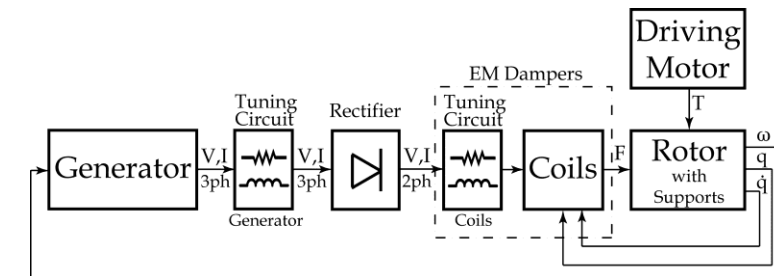
Figure 3: Block diagram of the self-powered magnetic damper system

3.2   Three Phase Generator

The equivalent circuit of the generator is reported in Figure 4. The voltages sources e_1, e_2, e_3 represent the back electromotive forces generated by each winding due to the angular speed, while resistors and inductors represent the total resistance and inductance of the winding and the tuning circuits (hence $R=R_m+R_{am}$ and $L=L_m+L_{am}$)

As it is well known from the field of permanent magnets synchronous machines, the total flux linking in the motor winding is the flux generated by the permanent magnets (λ_m) on the rotors summed to the flux of the self (L) and mutual (M) inductance of the windings:

$$\begin{cases} \lambda_1 = Li_1 + Mi_2 + Mi_3 + \lambda_{m1} \\ \lambda_2 = Mi_1 + Li_2 + Mi_3 + \lambda_{m2} \\ \lambda_3 = Mi_1 + Mi_2 + Li_3 + \lambda_{m3} \end{cases} \tag{1}$$

Considering, for instance, a star connection of the windings, the currents at node follows:

$$i_1 + i_2 + i_3 = 0 \tag{2}$$

The flux linkages (λ) of eq. (1) decouple form each other and can be rewritten in matrix form asthat can be rewritten in matrix form as:

$$\{\lambda\} = L_{eq}\{i\} + \{\lambda_m\} \tag{3}$$

where $L_{eq} = L - M$.
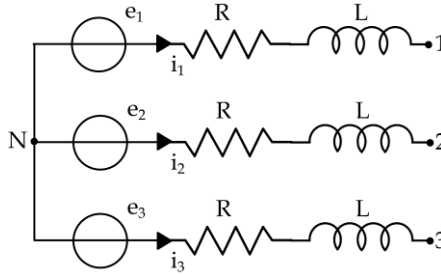
Figure 4: Equivalent circuit of the permanent magnet generator

The flux generated by the permanent magnets can be expressed by:

$$\{\lambda_m\} = \begin{Bmatrix} K\cos(\Theta) \\ K\cos\left(\Theta + \dfrac{2}{3}\pi\right) \\ K\cos\left(\Theta + \dfrac{4}{3}\pi\right) \end{Bmatrix} \tag{4}$$

Where $\Theta = p\Theta_m$ are the electrical angle, number of poles and mechanical angle ($\Theta_m = \Omega t$) respectively.

Referring to Figure 4, the expression of the line voltage is:

$$\begin{Bmatrix} v_{1N} \\ v_{2N} \\ v_{3N} \end{Bmatrix} = R\{i\} + \frac{d}{dt}\{\lambda\} \tag{5}$$

That, expanding the derivative can be rewritten as:

$$\{v_L\} = R\{i\} + L_{eq}\frac{d}{dt}\{i\} + \frac{d}{dt}\{\lambda_m\} \tag{6}$$

where the first term is the resistance voltage drop, the second is the inductance drop and the last if the back electromotive force.

Considering the time derivative of eq. (4) the back electromotive force is:

$$\{e\} = \frac{d}{dt}\{\lambda_m\} = \begin{Bmatrix} -Kp\Omega\sin(p\Theta_m) \\ -Kp\Omega\sin\left(p\Theta_m + \dfrac{2}{3}\pi\right) \\ -Kp\Omega\sin\left(p\Theta_m + \dfrac{4}{3}\pi\right) \end{Bmatrix} \tag{7}$$

Multiplying the eq. (6) by the current the power expression is obtained:

$$P = \{i\}^T \{v_L\} = \{i\}^T R\{i\} + \{i\}^T L_{eq} \frac{d}{dt}\{i\} + \{i\}^T \{e\} \tag{8}$$

Where the first term is the resistance losses, the second is linked to the inductance power and the last is the mechanical power here reported separately:

$$P_m = \{i\}^T \{e\} = \{i\}^T \frac{d}{dt}\{\lambda_m\} = \{i\}^T \frac{d}{d\Theta}\{\lambda_m\} p\Omega \tag{9}$$

Hence, the torque, assuming constant spin speed

$$T = p\{i\}^T \frac{d}{d\Theta}\{\lambda_m\} \tag{10}$$

To solve the dynamic problem of eq. (6), the voltages between points 1-2 and 2-3 (Figure 4) can be used together with eq. (2).

$$\begin{cases} v_{12} = v_{1N} - v_{2N} \\ v_{23} = v_{2N} - v_{3N} \\ i_1 + i_2 + i_3 = 0 \end{cases} \tag{11}$$

In matrices

$$\begin{Bmatrix} \dfrac{di_1}{dt} \\ \dfrac{di_2}{dt} \end{Bmatrix} = -\frac{R}{L_{eq}}\begin{bmatrix} 1 & 0 \\ 0 & 1 \end{bmatrix}\begin{Bmatrix} i_1 \\ i_2 \end{Bmatrix} +$$
$$+ \frac{Kp\Omega}{\sqrt{3}L_{eq}}\begin{bmatrix} 2 & 1 \\ -1 & 1 \end{bmatrix}\begin{Bmatrix} \cos\left(p\Theta_m + \dfrac{2}{3}\pi\right) \\ \cos(p\Theta_m) \end{Bmatrix} \tag{12}$$

Eq. (12) represent the dynamic electrical model of the generator while driven at speed ω. The resulting mechanical torque to be applied to the generator is represented by eq. (10).

3.3   Electromagnetic Dampers

Figure 5 shows the sketch of a "transformer" eddy current damper used for each of the two lateral axis of the support. The coils are supplied with a constant voltage and generate the magnetic field linked to the moving element (anchor). The displacement, with speed $\dot{q}$, of the moving part of the magnetic circuit changes the reluctance of the circuit itself and produces a variation of the flux linkage so generating a back-electromotive force and ultimately eddy currents in the coils. The current in the coils has two contributions: a fixed one due to the voltage supply, and a variable one induced by the back electromotive force. The first contribution generates a force increasing with decreasing airgap, thus producing a negative stiffness. The damping force is generated by the second contribution, acting against the speed of the moving element. It is a semi-active device, which requires power to generate the magnetic field. The voltage in the coil may be changed to vary the performance. Once the voltage is kept constant, there is no need of closed-loop position feedback and sensors are not required.
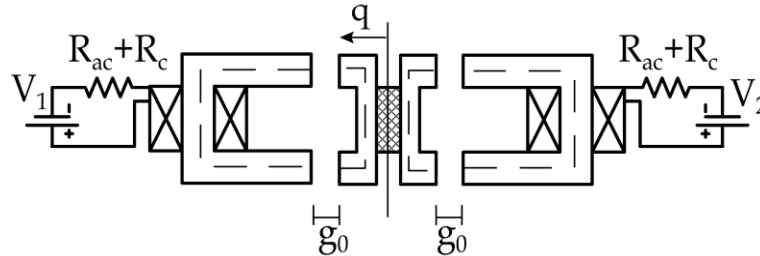
Figure 5: Sketch of a two electromagnet Semi Active Magnetic Damper (the elastic support is omitted).

Energy dissipation takes place in the stator, so that the device supplies non-rotating damping. The transfer function between the speed $\dot{q}$ and the electromagnetic force F shows a first order dynamics with pole frequency ω_{RL} due to the R-L nature of each circuit

$$\frac{F}{\dot{q}} = \frac{1}{s} \frac{K_{em}}{\left(1 + s/\omega_{RL}\right)}$$ (13)

where $K_{em} = -\dfrac{2V^2/R}{q_0^2 \omega_{RL}}$ is the negative stiffness coefficient, $\omega_{RL} = \dfrac{R}{L_0}$, $L_0 = \dfrac{\mu_0 N^2 A}{2q_0}$. The term V is the constant voltage supplied to the electromagnet and R the total resistance of the device (R=Rc+Rac). The additional resistance Rac can be used to modify the damping.

Due to the factor $1/s$, and the negative value of K_{em}, the mechanical impedance is that of a band limited negative stiffness. The value of the negative stiffness is proportional to the electrical power dissipated at steady state by the electromagnet. For given values of the number of turns of the windings (N), of the airgap area (A), and clearance (q_0), the mechanical impedance and the pole frequency are functions of the voltage supply V and the resistance R . The negative stiffness prevents the use of the electromagnet driven by constant voltage to support the rotor unless the excitation voltage is controlled by a fast active feedback that compensates it. A very simple alternative to the active feedback is to put a mechanical spring, of stiffness K_m, in parallel to the electromagnet. To avoid static instability, the stiffness K_m of the added spring has to be larger than the negative electromechanical stiffness of the damper ($K_m \geq -K_{em}$). In the case of an already supported structure it could be possible to utilize the mechanical stiffness of the structure itself. Alternatively, an additional spring system could be introduced into the support structure in parallel to the damper. As a matter of fact, this spring can be considered as part of the damper.

Due to the essential role of the spring the impedance of eq.(13) is not very helpful in understanding the consequences of including a transformer damper into a mechanical structure. Instead, a better insight can be obtained by studying the mechanical impedance of the damper in parallel with the mechanical spring, i.e. of the damper:

$$\frac{F}{\dot{q}} = \frac{1}{s}\left(\frac{K_{em}}{\left(1 + s/\omega_{RL}\right)} + K_m\right) = \frac{K_{eq}}{s}\frac{1 + s/\omega_z}{1 + s/\omega_{RL}}$$ (14)

where $K_{eq} = K_m + K_{em}$; $\omega_z = \omega_{RL}\dfrac{K_{eq}}{K_m}$.
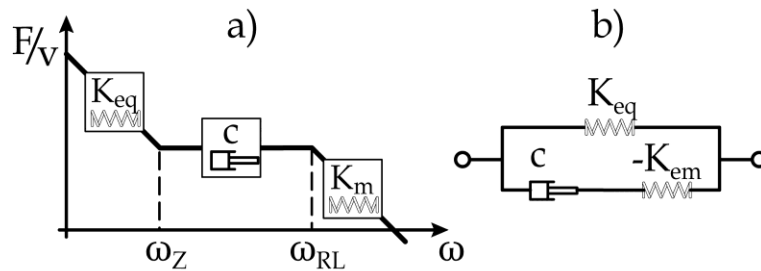
Figure 6: a) mechanical impedance of a transformer eddy current damper in parallel to a spring of stiffness K_m. b) Mechanical equivalent

Apart from the pole at null frequency, the impedance shows a zero-pole behaviour. Since to ensure stability $0 < -K_{em} < K_m$, the zero frequency (ω_z) must be smaller than the pole frequency ($0 < \omega_z < \omega_{RL}$). As shown in Figure 6.a, it is possible to identify three different frequency ranges:

- Equivalent stiffness range $\omega << \omega_z < \omega_{RL}$ the system behaves as a spring of stiffness $K_{eq} > 0$.

- Damping range $\omega_z < \omega < \omega_{RL}$ the system behaves as a viscous damper with coefficient

$$C = \frac{K_m}{\omega_{RL}} \tag{15}$$

- Mechanical stiffness range $\omega_z < \omega_{RL} << \omega$ the transformer damper contribution vanishes and the only contribution is that of the mechanical spring of stiffness K_m.

It is interesting to note (Figure 6.b) that the resulting model is the same as Maxwell's model of viscoelastic materials [19]. At low frequency the system is dominated by spring K_{eq} while the lower arm of the parallel in 6.b does not contribute. At high frequency the viscous damper "locks" and the stiffnesses of the two springs add. The viscous damping dominates at intermediate frequency.

A detail description of the equations at the base of the models presented in this section is reported in [15]

3.4   Mechanical System (Plant)

The mechanical part of the system consists in the rotor and it supports (springs). The model describes only the lateral behaviour. Axial and torsional behaviour is not considered here as it is decoupled from the lateral. The main hypotheses are constant spin speed, small rotation (except for spinning) and displacements.

The equation of motion used for the rotor model is described in terms of the nodal displacements vector $\mathbf{q}$ as:

$$\mathbf{M}_{xy}\ddot{\mathbf{q}}_{xy}(t) + \left(\mathbf{L}_{xy} + \Omega\mathbf{G}_{xy}\right)\dot{\mathbf{q}}_{xy}(t) + \left(\mathbf{K}_{\Omega 0 xy} + \Omega^2\mathbf{K}_{\Omega 2 xy} + \Omega\mathbf{H}_{xy}\right)\mathbf{q}_{xy}(t) =$$

$$= \mathbf{f}_{sxy} + \Omega^2\mathbf{f}_{umb}\begin{Bmatrix}\sin(\Omega t)\\\cos(\Omega t)\end{Bmatrix} + \mathbf{S}_{ixy}\mathbf{f}_{xy}(t) \tag{16}$$

A detailed description of the behaviors of rotor can be found in [15]

The rotor shaft has been modeled using a FE code as a series of 21 nodes and 20 Timoshenko beam elements; the disks have been modeled as two lumped masses that take into account also the inertia properties. Thus the model advised has gyroscopic effects that cannot be neglected. The rotor is modeled as free-free, hence the supports have to be inserted into the model as separated components and modeled simply as springs.

4   System Design and Performances

The parameters of the system have been designed and performances have been evaluated using the previously described model implemented in the time-domain simulator.

The first step is the definition of parameters of the electromagnetic damper. To this end, considering the electrical properties of the coils and the dynamics (second critical speed) of the mechanical system that has to be damped, the value of the additional resistance and the supply voltage of the coils can be chosen. Usually the R-L pole of the coil is placed close to the mechanical resonance; due to design constraint and to the availably of the components a slightly lower frequency has been selected (240rad/s instead of the 390 rad/s of the second critical speed); this leads to a lower performing electromagnetic damper but allows an easier implementation. As the rated performance are modelled no generality in the approach is lost.

In this way, the electromagnetic damper circuit is defined and can be considered as a "load" for the generator unit. To identify the best values for the tuning inductance and resistance (L$_{am}$, R$_{am}$) a parametric analysis, has been performed.

Figure 7 and Figure 8 show the behaviour of the generator torque and power respectively for different values of the tuning inductance Lam. The torque has a peak corresponding to the electrical pole of the generator and tuning circuit with the effect that, increasing the inductance, the peak amplitude decreases. This property allows to cope with the need of limiting the adsorbed damping power (and damping effect) above a selected spin speed.

Figure 9 show the voltage at the output of the diodes rectifier, which is the supply all four damper's coils (all of them are connected in parallel). In addition, in this case the voltage is no longer increasing after the generator electrical pole.
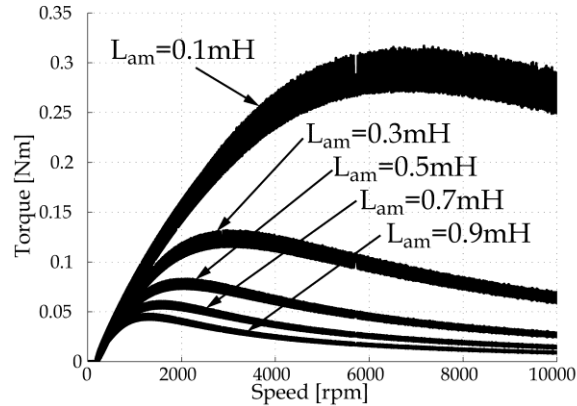
Figure 7: Required torque to drive the generator with different tuning circuit inductances
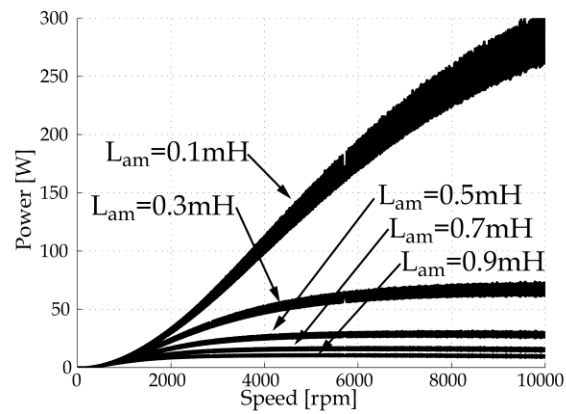
Figure 8: Required power to drive the generator with different tuning circuit inductances
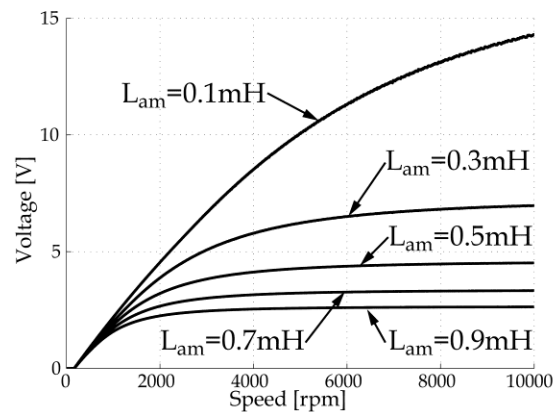
Figure 9: Electromagnetic damper coil voltage with different tuning circuit inductances

The selection of the tuning inductance is a compromise between the voltage (related to the damping effect) and the spin speed where the voltage is no longer increasing. Figure 9 shows that increasing L_{am} reduces both the voltage and the level-off speed. The first should be as higher as possible while the second should be close to the critical speed. In the present case a value of about Lam=0.5mH has been adopted to reach a voltage of about 4.5V for speeds larger than 3500rpm. This voltage is what required to ensure the performances of the electromagnetic damper.

5   Experimental Validation

An intensive validation test campaign has been carried on to evaluate some parameters needed for the design (i.e: the generator winding inductance) and to identify some unknown the characteristics required for tuning the models and finally to validate the performances of the full system.

5.1   Three Phase Generator

Coil resistance and the voltage constant are usually available in datasheet. As the whole system is sensitive to the generator parameters, they have been characterized experimentally to improve the reliability of the model. DC resistance is easily measured by means of an impedance-meter and reported in Table 2.The voltage constant has been measured driving the generator in open circuit and measuring the phase to phase voltages at various spin speed. Figure 10 shows the voltages waveform acquired compared to the ones resulting from the generator model. The identified value is reported in Table 2 and shows a difference of about 10% from the datasheet.
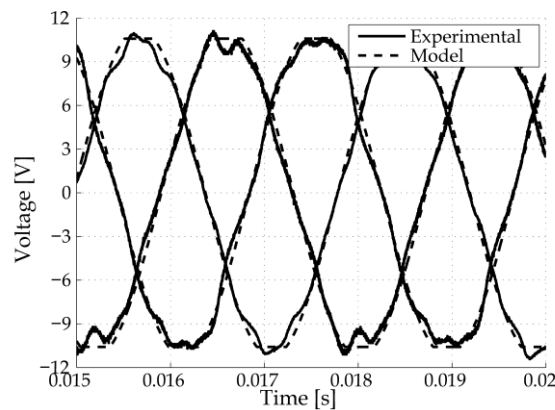
Figure 10: BEM voltage evaluation during no load operation of the generator

The winding inductance is not usually provided with datasheet even if it is an essential parameter for designing the damper. To evaluate that value a specific test bench has been devised. Another electrical motor (of know torque characteristic) has been used to drive the generator that was, this time, shorted on its windings. The generator has been spun up through the operating range while measuring the current employed from the driving motor. In the lack of a dedicate torque-meter the corresponding torque has been evaluated form the motor torque constant. The resulting torque to speed characteristic of the short-circuited generator is reported in Figure 11.
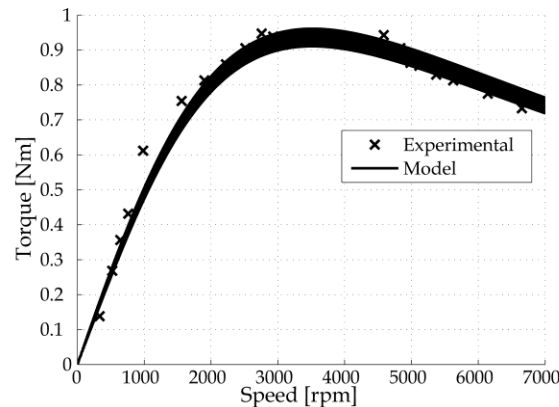
Figure 11: Torque characteristic of the short-circuited generator

The same test has been performed using the dynamic simulator varying the value of the coils inductance to obtain the best fit with the experimental identify the most suitable value that cope with the experimental data.

5.2   Electromagnetic Dampers and Mechanical System

The electromechanical part has been tuned and validated before running the damping system in the self-powered configuration. The variation of the damper inductance due to the anchor displacement mainly influences the behaviour of the electromagnetic damper. To better tune the model, this characteristic has been measured evaluating the inductance of each coil while varying its airgap (Figure 12). The fitted ("power type" y=a*x^b+c) characteristic of the mean values is then used in the models.
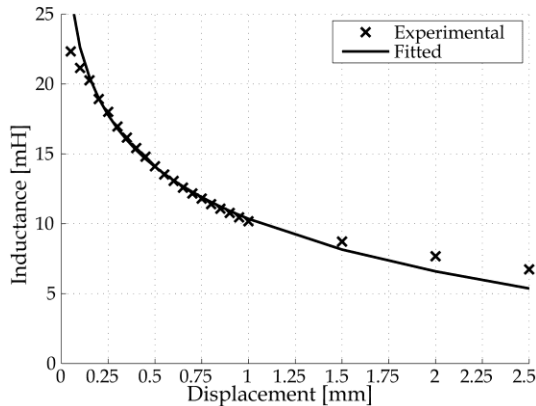
Figure 12: Fitting of the electromagnetic damper coil inductance
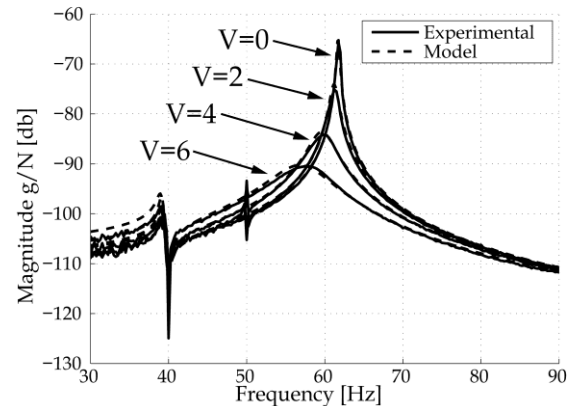
Figure 13: FRF of the rotor (standstill) at various supply voltage

The validation of the damping characteristic has been performed by comparing the transfer function (FRF) between the input force and the output acceleration obtained from the experimental tests and that computed with the model. Damping circuit has been supplied, in this phase, with a constant voltage at null angular speed of the rotor. The input force was actuated by means of an instrumented hammer; the acceleration was measured using an accelerometer. The impact point and the accelerometer are close to the damper bearing housing. A first series of tests was performed with null excitation voltage to evaluate the structural damping of the structure. The transfer functions obtained from the model are then compared in Figure 13 to the experimental ones for various excitation voltages Hidden lines in the figure indicate the results from the model while the solid ones refer to the experimental results. The correlation between the numerical and experimental results confirms the validity of the adopted modelling approach and of the underlying assumptions. As predicted by the model, increasing the voltage supply increases the damping range of the transformer damper. Even if the damping is increased at the cost of a reduction of the resonant frequency, the large added damping demonstrates the effectiveness of the damper.

5.3   Self-Powered Damper performance

The validation of the whole system has been performed with a slow run-down test from 6000rpm to null spin speed. To show the effectiveness of the damping system the first test is performed with the damping device in open circuit condition to obtain null added damping then the self-powered damper is switched on to show its effect. During these tests the main rotordynamics values (vibrations and currents in coils) have been acquired. Figure 14 show the comparison between the estimated (model) and measured coil current during the test showing a good agreement between the two.
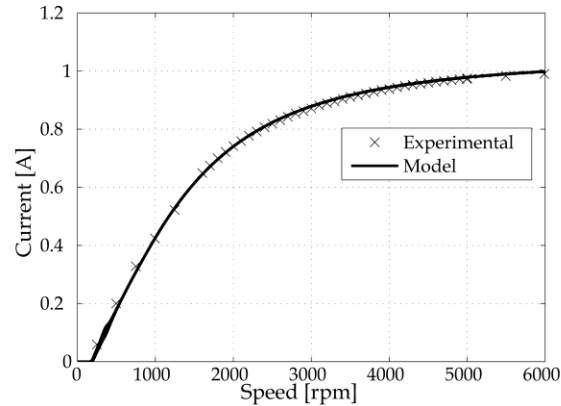
Figure 14: Measured and estimated coil current during the run-down test

Figure 15 shows the unbalance response while the damping system is switched off. The model is computed using the identified unbalance level and reports the two critical speed crossing due to the vibration of the rotor relative to the supports. The first critical speed involves mainly the undamped support, while the second involves the support with the self-powered damper. The agreement between the experiment and the model, on both axis, is good even if, as the system presents a really small damping, the tuning in the peak value is quite hard. Furthermore the plant shows a little anisotropy that is not fully taken into account during modelling. The experimental data have been acquired with a couple of eddy current position sensors, processed in order to remove the mechanical run-out and filtered to include only the synchronous component of the vibration. The experimental not taken into account by the model can be due to electrical disturbance.

Figure 16 reports the results when the self-powered magnetic damper is activated. The experimental results show with good agreement with the results of the simulation. The effect of the added damping is clearly visible. As with the result at standstill (FRF) the damper, due to the negative stiffness added by the electromagnets, causes a slight reduction of the critical speed. Also in this case the experiments results are not reported for the first critical speed because the dampers are not activate on the other support and it has not been tuned.
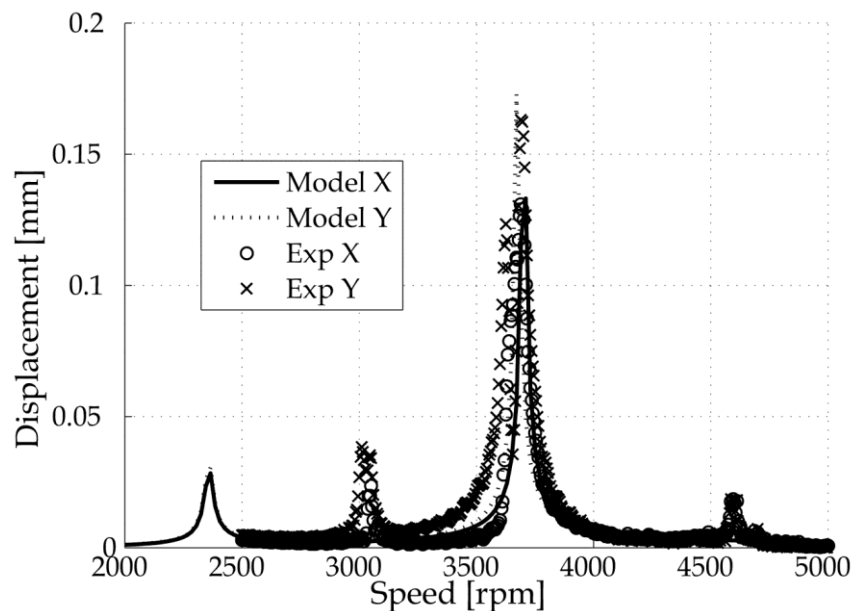
Figure 15: Unbalance response with the electromagnetic damping device disabled
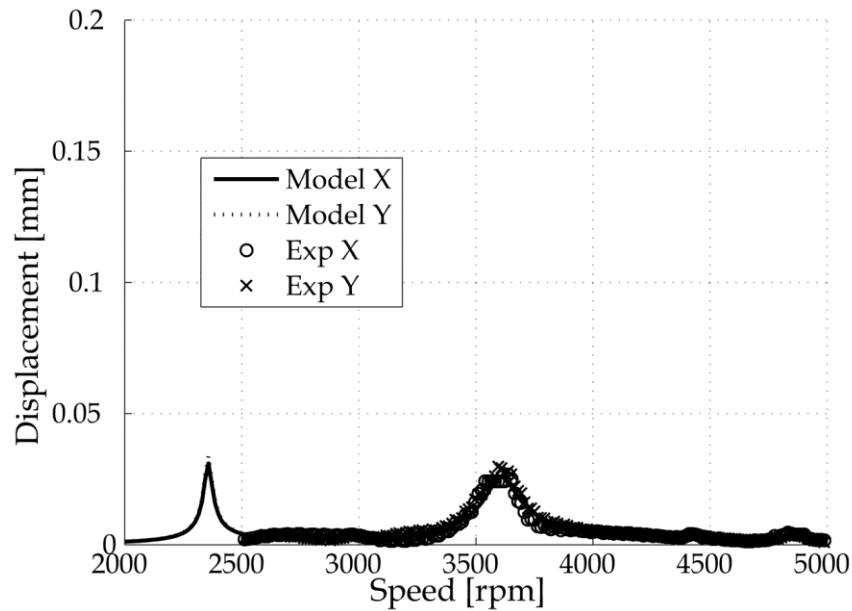
Figure 16: Unbalance response with the self-powered electromagnetic damper enabled

6   Conclusion

The present paper studies the feasibility and evaluates the performances of an electromagnetic damper, with its own self-powering supply system to be used in vibration control of rotors.

A laboratory rotordynamic test bench, representative of a scaled low-pressure civilian aero-engine, has been used to develop and validate the proposed device.

Beside the analytical formulation of the generator and the electromagnetic damping devices, a numerical model of the whole system has been developed and tuned.

The design procedure starting from the parameters of each single subsystem has been presented and then experimentally validated.

The experimental tests have been performed both to identify the unknown parameters and to validate the model assumptions and methodologies adopted

Experimental results show a good agreement with the models and demonstrate the effectiveness of the proposed device.

As main constrains of the present design come from the requirements of using components of the shelf (generator, tuning coils), general performance, in terms of achievable damping and efficiency of the system can be improved. Hence a careful design of the generator together with the electric parameters design of the damping actuator can lead to a smaller and more performing self-powered electromagnetic damper

Acknowledgements

References

[1]   Y. K. Ahn, B-S. Yang, S. Morishita, 2002, "Directional Controllable Squeeze Film Damper Using Electro-Rheological Fluid", ASME Journal of Vibration and Acoustics, vol. 124, pp. 105-109.

[2]   J. M. Vance, D. Ying, 2000, "Experimental Measurements of Actively Controlled Bearing Damping with an Electrorheological fluid", ASME Journal of Engineering for Gas Turbines and Power, vol. 122, pp 337 - 344.

[3]   J. Meisel, 1984, *Principles of Electromechanical Energy Conversion*, Robert Krieger, Malabar, Florida.

[4]   S. H. Crandall, D. Karnopp, E. F Kurtz, E. C. Pridmore-Brown, 1968, *Dynamics of Mechanical and Electromechanical Systems*, New York: McGraw-Hill.

[5]   K. E., Graves, D. Toncich, P. G. Iovenitti, 2000, "Theoretical Comparison of the Motional and Transformer EMF Device Damping Efficiency" Journal of Sound and Vibration, Vol. 233, No. 3, pp 441-453.

[6]   A. Tonoli, N. Amati, M. Padovani, 2003, "Progetto di Smorzatori e Giunti Elettromagnetici per Alberi a Gomiti", *Proceedings of the XXIII AIAS Conference*, Salerno, 3-6.

[7]   K. Nagaya, 1984, "On a Magnetic Damper Consisting of a Circular Magnetic Flux and a Conductor of Arbitrary Shape. Part I: Derivation of the Damping Coefficients", Journal of Dynamic Systems, Measurement and Control, vol. 106, pp. 46-51.

[8]   K. Nagaya, Y. Karube, 1989, "A Rotary Magnetic Damper or Brake Consisting of a Number of Sector Magnets and a Circular Conductor", Journal of Dynamic Systems, Measurement and Control, vol. 111, pp. 97-104.

[9]   D. Karnopp, 1989, "Permanent Magnets Linear Motors used as Variable Mechanical Damper for Vehicle Suspension", Vehicle System Dynamics, vol. 18, pp. 187-200.

[10] D. Karnopp, D. L. Margolis, R. C. Rosenberg, 1990, *System Dynamics: a Unified Approach*, J. Wiley & Sons.

[11] Y. Kligerman, O. Gottlieb, 1998, "Dynamics of a Rotating System with a Nonlinear Eddy-Current Damper", ASME Journal of Vibration and Acoustics, Vol. 120, pp. 848-853.

[12] Y. Kligerman, A. Grushkevich, M. S. Darlow, 1998, "Analytical and Experimental Evaluation of Instability in Rotordynamics System with Electromagnetic Eddy-Current Damper", ASME Journal of Vibration and Acoustics, Vol. 120, pp. 272-278.

[13] A. Tonoli, 2007, "Dynamic characteristics of eddy current dampers and couplers", Journal of Sound and Vibration, vol. 301, pp. 576-591.

[14] N. Amati, A. Festini, A. Tonoli, 2011, Design of electromagnetic shock absorbers for automotive suspensions, Vehicle System Dynamics, vol. 49 n. 12, pp. 1913-1928. - ISSN 0042-3114

[15] N. Amati, M. Silvagni, A. Tonoli, Transformer eddy current dampers in rotating machines vibration control, Journal of Dynamic Systems, Measurement, and Control, May 2008, Vol. 130 / 031010-1

[16] Tonoli A., Amati N., Bonfitto A., Silvagni M., Staples B., Karpenko E, Design of Electromagnetic Dampers for Aero-Engine Applications, Journal of Engineering for Gas Turbine and Power, 2010, , vol. 132 n. 11, ISSN 0742-4795. (2010)

[17] Tonoli A., Silvagni M., World Patent N.WO2010133333, Electromagnetic damper for rotating machines

[18] G. Genta, 2004, Dynamics of Rotating Systems, Springer Verlag.

[19] D.F. Golla, P.C. Hughes, Dynamics of Viscoelastic Structures--A Time Domain, Finite Element Formulation, Journal of Applied Mechanics, December 1985, Vol. 52, pp. 897-906.